ISSN 1063-7834, Physics of the Solid State, 2022, Vol. 64, No. 12, pp. 616–623. © Pleiades Publishing, Ltd., 2022.
Russian Text © The Author(s), 2021, published in Khimicheskaya Fizika i Mezoskopiya, 2021, Vol. 23, No. 2, pp. 165–175.

Conduction Mechanisms and Thermoelectric Properties of Semimetallic CaSi and $CaSi_2$ Films on Si(100) and Si(111) Substrates

N. G. Galkin[a, *], K. N. Galkin[a], A. V. Tupkalo[a], E. Yu. Subbotin[a], I. M. Chernev[a], A. V. Shevlyagin[a], and V. V. Khovailo[b]

[a] *Institute of Automatics and Controlling Processes, Far-Eastern Branch, Russian Academy of Sciences, Vladivostok, 690041 Russia*

[b] *National Research Technological University MISiS, Moscow, 119991 Russia*

**e-mail: ngalk@iacp.dvo.ru*

Received March 4, 2021; revised June 27, 2021; accepted June 27, 2021

Abstract—Nanocrystalline CaSi films with thicknesses from 80 to 130 nm were grown on high-resistance silicon substrates with orientations (111) and (100) by the methods of low-temperature (190–330°C) molecular-beam epitaxy and low-temperature (330°C) solid-phase epitaxy, for which the microstructure, phase composition, and crystal structures were studied. It is found that the polycrystalline, nanocrystalline (NC), and amorphous CaSi and $CaSi_2$ films are characterized by preferential contribution of holes in the range 1.4–300 K. In magnetic fields 1–4 T and at temperatures 40–100 K, a giant linear magnetoresistive effect (MRE) (to 500%) was observed for the first time in CaSi films with the contribution of another $CaSi_2$ phase. In $CaSi_2$ film containing another phase (CaSi), peaks are detected on the temperature dependences of the resistivity and the Hall coefficient that correspond to a phase transition. In addition, in this film, the transition from the positive MRE to negative MRE is observed at $T = 120$–200 K. This effect is not observed in the single-phase $CaSi_2$ film, which corresponds to a certain reconstruction of carrier flows in a magnetic field only in the two-phase system. The study of the thermoelectric properties of CaSi and $CaSi_2$ films shows that the semimetallic type of the conduction in them leads to the independence of the positive Seebeck coefficient $T = 330$–450 K. It is found that the maximum contribution to the Seebeck coefficient and the power factor are observed in the amorphous CaSi film in the case of the presence of some fraction of NC Ca_2Si phase. In the single-phase $CaSi_2$ films, the Seebeck coefficient and the power factor are halved due to an increase in the hole concentration as compared to the CaSi films.

Keywords: semimetallic films, CaSi, $CaSi_2$, conduction mechanism, semimetal–semiconductor transition, giant magnetoresistance, thermoelectric properties, power factor

DOI: 10.1134/S1063783422120034

INTRODUCTION

Calcium silicides are ecologically pure materials and they occupy a specific place among alkali-earth metal silicides. This fact is related, first, with a wide set of properties of calcium silicides (Ca_2Si, CaSi, Ca_3Si_4, Ca_5Si_3, $Ca_{14}Si_{19}$, and $CaSi_2$ [1]) from semiconducting [2] to semimetallic [3]. It can lead to their wide application in various fields of engineering and electronics. Such a wide spectrum of the properties and possible applications is related to a fine tuning of the electron system of calcium silicides as the silicon concentration increases and the fraction of the covalent and ionic bond in them is changed due to involving of Ca *d* electrons to the bond with silicon [3, 4]. However, the physical properties of bulk and film semimetallic silicides are scantily known [5, 6]. The transport properties of calcium monosilicide (CaSi) films were studied before only after developing the method of their formation on silicon [7, 8], but the magnetotransport and thermoelectric properties were not studied in detail [9]. In this connection, the necessity arises to systematically study the electrical properties of the CaSi films using the Hall, magnetoresistive, and thermoelectric measurements of variable temperature, the comparison of them with the data on the morphology and the structure of the grown films to determine the main mechanisms of formation of the conduction of nanocrystalline CaSi films and the contribution of additional silicide phases to the formation of the magnetoresistance value, the Seebeck coefficient, and the power factor in CaSi films.

Table 1. Parameters of samples and substrates; growth and characterization methods of films

Sample	Substrate, type	Resistivity (Ω cm)	Growth method, substrate T, °C/annealing T, °C	XRD data [8, 9]	Method of electrical measurements	
					LT Hall, LT MR	HT Zeebeck effect
A	Si(100), FZ	2000	SPE, 20/330	CaSi(220) + (polycrystalline) + Ca_2Si (amorphous)	No	Yes
B	Si(100), FZ	2000	MBE, 330/330	CaSi + $CaSi_2$ (weak), polycrystalline	Yes	Yes
C	Si(100), FZ	2000	MBE, 500/20	hR3 $CaSi_2$(0001) + CaSi(010)	Yes	Yes
D	Si(100), FZ	2000	MBE, 500/20	hR3 $CaSi_2$(0001) + CaSi(010)	No	Yes
E	Si(111), KDB	45	MBE, 190/300	CaSi(200), nanocrystalline + amorphous	No	Yes
F	Si(100), FZ	2000	MBE, 320/20	CaSi[(111), (004), (122), (220), (131)	No	Yes
G	Si(100), FZ	2000	MBE, 500/20	hR6 $CaSi_2$(010) + CaSi	No	Yes
H	Si(111), KDB	45	MBE, 320/20	CaSi(004), CaSi(200) polycrystalline	Yes	Yes
I	Si(111), KDB	45	MBE, 500/20	hR3 $CaSi_2$(0001) + hR6 $CaSi_2$(0001)	Yes	Yes

The high-temperature thermoelectric and resistive measurements allow us to estimate the mechanism of the thermoelectric generation in the grown CaSi films and to estimate the perspectives of their applying as branches of a thermoelectric transducer.

To study the conduction mechanisms in semimetallic calcium silicides, we grew, on silicon substrates with two orientations Si(111) and Si(100), a number of samples with calcium silicide films of two main compositions CaSi and $CaSi_2$ that were studied before using the structural, optical spectroscopic method and, previously, by electrical methods [8, 10]. Since mainly two-phase systems formed at low growth temperatures (300–500°C), it was necessary to systematically study the electrical properties of these films by the low-temperature methods of Hall, magnetoresistive, and thermoelectric measurements comparing them with the data on the morphology and the structure of the grown films.

EXPERIMENTAL

The Ca silicide films were grown in a ultrahigh-vacuum chamber of an OMICRON installation with a base vacuum of 1×10^{-10} Torr equipped by a block of molecular-beam sources of silicon (Si) and calcium for the co-deposition of Ca and Si on Si(100) and Si(111) substrates at fixed temperatures from 20°C to 500°C. The rectangular p-Si strips (4×12 mm^2) with the resistivities 45 and 2000 Ω cm were used as the substrates and also as silicon sublimation sources. A Knudsen cell with a crucible made of pyrolitic boron nitride, a tungsten heater, a tantalum screens, and a small Ca weight (about 10–15 mg) in the crucible was used as a Ca atom source. In both evaporators, the Ca and Si deposition rates were calibrated be a quartz thickness sensor. They were 2.5–5.5 and 0.8–1.5 nm/min for calcium and silicon, respectively, in variouth growth experiments. Nine samples with Ca silicide films were grown by the solid-phase epitaxy (SPE) or by molecular-beam epitaxy (MBE) at various temperatures and additional annealings (sometimes) (Table 1). The measuring techniques are described in [8–10].

RESULTS AND DISCUSSION

Morphology and Structure of Calcium Silicide Films on Silicon

Consider the peculiarities of the morphology of the grown films. Figures 1a–1i show the images of the surfaces of the film grown on the substrates of two types (FZ-2000 and KDB-45) at various temperature conditions described in Table 1.The calcium monosilicide (CaSi) films in samples **A**, **E**, **F**, and **H** formed at temperatures 190–300°C by SPE and MBE have the most disordered structure and morphology (Figs. 1a, 1e, 1f, and 1h). The film in sample **A** on the Si(100) substrate (Fig. 1a) consists of randomly oriented grains of the rectangular and triangular shapes with sizes 200–

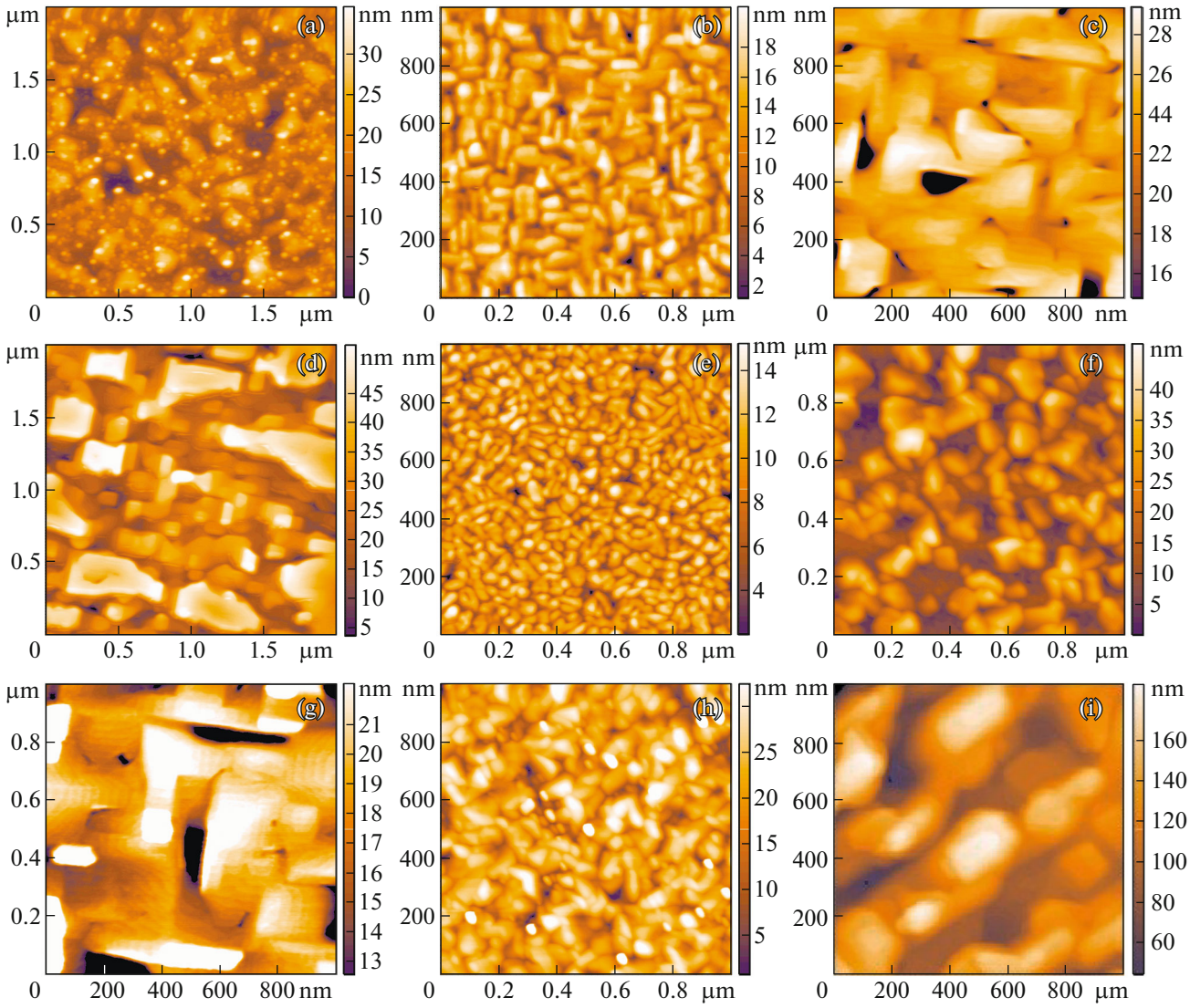

Fig. 1. Pictures of the surface of calcium silicide films obtained by the semicontact method of atomic force microscopy (AFM): (a) sample **A**; (b) sample **B**; (c) sample **C**; (d) sample **D**; (e) sample **E**; (f) sample **F**; (g) sample **G**; (h) sample **H**; (i) sample **I**.

300 nm and small islands (20–40 nm) covering them, which determines an increased roughness of the film (σ_{rms} = 5.49 nm). In sample **E**, there are fine grains with sizes 40–60 nm partially disposed at angles ±60° (Fig. 1e) and insignificant roughness (σ_{rms} = 2.09 nm), which is determined by the orienting influence of the substrate with orientation (111). In sample **F**, the film appears structurally discontinuous with a strong roughness (σ_{rms} = 9.39 nm) and consists of unjoined grains with oval shape (Fig. 1f) that have only the CaSi structure (Table 1). In sample **H**, the film grown on the Si(111) substrate (Fig. 1h) has a developed morphology and consists of fine and rough grains with sizes 20–80 nm without certain orientation with respect to the substrate and with marked roughness (σ_{rms} = 6.64 nm). The film in sample **B** (Fig. 1b) grown at 330°C and additionally annealed at T = 330°C has the most ordered structure with roughness σ_{rms} = 3.12 nm consisting of mutually perpendicular faceted CaSi grains (Table 1). In this case, another calcium disilicide ($CaSi_2$) is not identified by the morphology data, according to [9]. The $CaSi_2$ films in samples **C**, **D**, **G**, and **I** formed by MBE method at 500°C have an ordered structure (Figs. 1c, 1d, 1h, and 1i) and a medium roughness (σ_{rms} = 4.3–33.7 nm). On the substrate with orientation (100), they consist of mutually perpendicular rectangular grains with sizes 100–400 nm; on the substrate with orientation (111), they also consist of joined rectangular grains with the mutually perpendicular orientation but rotated at 45° with respect to the substrate.

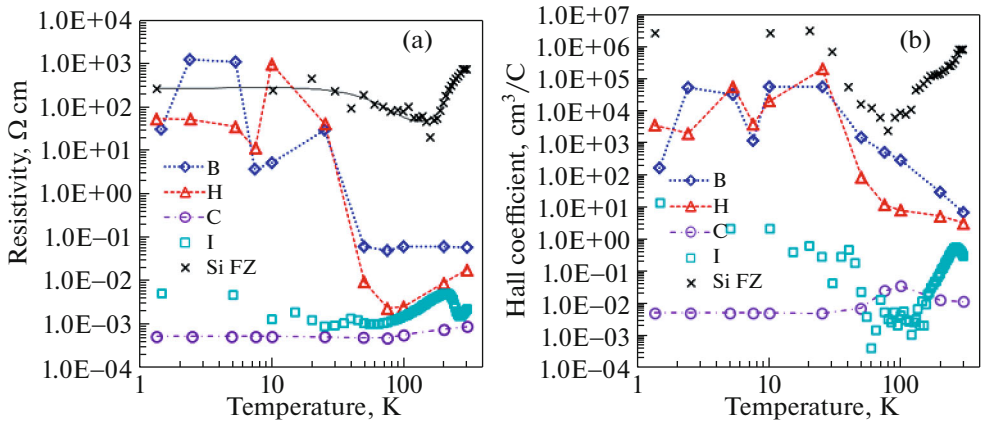

Fig. 2. Temperature dependences (on a full logarithmic scale) of (a) resistivity and (b) Hall coefficient for nanocrystalline CaSi films (samples **B** and **E**), and Si substrate (Si-FZ). Substrate resistivity (a) fits well with power law $y = bT^6$.

Low-Temperature Hall Effect in Nanocrystalline CaSi and $CaSi_2$ Films

Consider the low-temperature data of the Hall measurements on CaSi films (samples **B** and **H**) and films $CaSi_2$ (samples **C** and **I**) grown on two types of silicon substrates (Si(100) FZ and Si(111) KDB-45) and compare them with the morphology (Fig. 1) and structural (Table 1) data for them. According to the data of the Hall measurements (Fig. 2a), in the temperature range 50–300 K, the resistivity of the film in sample **H** is almost one order of magnitude lower than that of the film in sample **B**. Since the resistivity of the substrates is substantially higher than that of the films, there is no shunting at $T = 50$ K and higher. This fact is also confirmed by the data for the temperature dependences of the Hall coefficients for samples **B** and **H** and the silicon substrate (Fig. 2b). At temperatures lower than 50 K, the resistivity of both the films increases by 3–4 orders of magnitude (Fig. 2a), which correlates with the increase in the Hall coefficient (Fig. 2b) that is inversely proportional to the main carrier concentration. The calculations of the effective parameters in samples **B** and **H** without considering the shunting of the substrates at temperatures 50–300 K show that the main carriers in these films are holes with concentration 10^{16}–10^{18} cm^{-3} and the effective mobility120–200 $cm^2/(V s)$ at $T = 300$°C. At temperatures 50–25 K, the film resistivity significantly increase, which correlates with a decrease in the hole concentration. Since CaSi is a semimetal with two types of carriers with the same concentrations in the pockets near the Fermi level, according to the data of the theoretical calculations [11], the decrease in the hole concentration can be due to a motion of the Fermi level toward the electron pocket and a decrease of the hole contribution because of a violation of the compensation in the films. At temperatures near 7.5 K, the resistivity (Fig. 2a) and the Hall coefficient (Fig. 2b) have minima which can be related to collective effects: charge density wave in magnetic field [12].

In $CaSi_2$ films in samples **C** and **I**, we observe another type of the temperature dependences of the resistivity (Fig. 2a) and the Hall coefficient (Fig. 2b) (according to [11]). The films are not shunted over entire temperature range from 1.4 K to 300 K. In this case, the resistivity of sample **C** smoothly decreases and saturated at temperatures lower than 100 K. Conversely, the temperature dependence of the Hall coefficient has a local maximum near 100 K with further its decrease and saturation below 25 K (Fig. 2b). The more complex temperature dependence of the resistivity (Fig. 2a) and the Hall coefficient (Fig. 2b) is observed for sample **I.** The resistivity has one noticeable ($T = 200$ K) and two low ($T = 40$ K and $T = 15$ K) maxima. The Hall coefficient has a high maximum at $T = 250$ K, the subsequent minimum near 100 K, and then it smoothly increases (Fig. 2b). The calculations of the effective parameters in samples **C** and **I** without considering the shunting by the substrates at temperatures 250–300 K show that the main carriers in these films are holes with concentration 2×10^{19}–5×10^{20} cm^{-3} and the effective mobility 20–130 $cm^2/(V s)$ at $T = 300$°C. According to the theoretical calculations [7], $CaSi_2$ is also a semimetal with two types of the pockets in the Brillouin zone. Thus, the existence of peaks in the temperature dependences of the resistivity and the Hall coefficient in the $CaSi_2$ films (Fig. 2) can be determined by the formation of phase transitions in stressed grains.

Magnetoresistive Properties of CaSi and $CaSi_2$ Films on Silicon

The complex character of the low-temperature conductivity and the existence of strong inhomogeneities were studied additionally by the transverse magnetoresistance method in the temperature range 1.4–

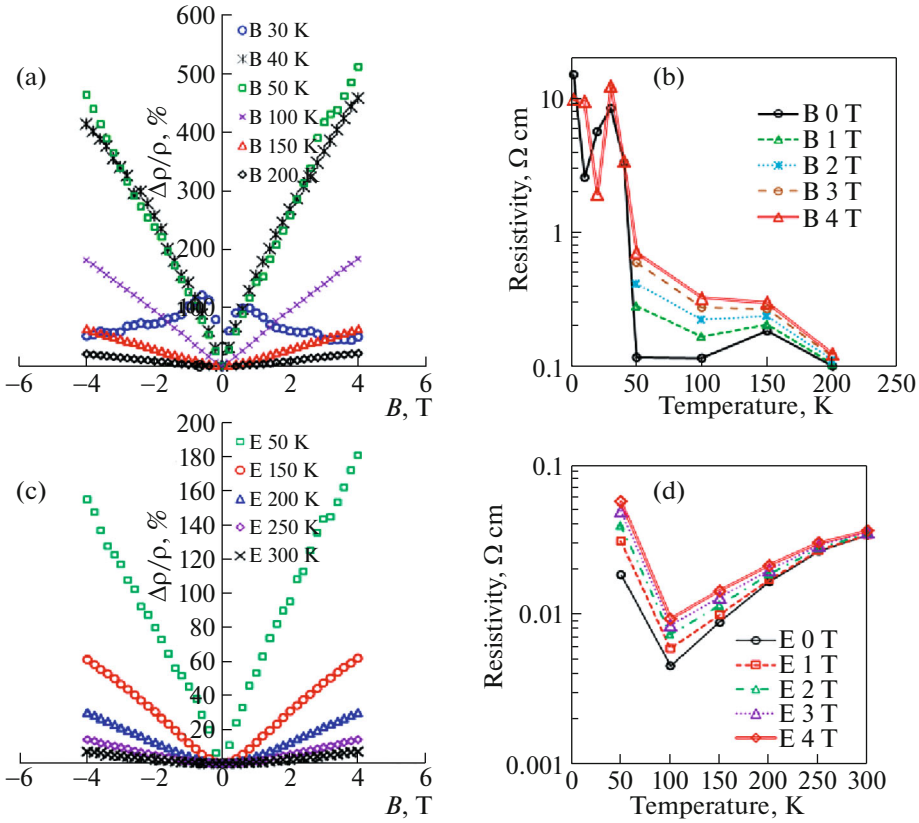

Fig. 3. (a, c) Dependences of the relative change in the magnetoresistance (Δρ/ρ) of the CaSi films on the magnitude of the magnetic induction at two directions of the magnetic field and (b, d) the specific resistance of the CaSi films on temperature in a zero magnetic field and in a magnetic field with induction from 1 to 4 T in samples **B** and **E**.

300 K and in magnetic fields from –4 to +4 T. Figures 3a–3d depict the dependences of the relative change in the magnetoresistance (Δρ/ρ) (Figs. 3a, 3c) of the films on the magnetic induction at two directions of a magnetic field and the changes in the resistivity of the films in a zero and nonzero magnetic fields for the CaSi films in samples **B** and **E**. At the minimal temperature 1.4 K, the film resistivity in sample **B** is not dependent on the magnetic field; thus, the value of Δρ/ρ is zero. The dependence on magnetic field appears at $T = 30$ K, but its shape is not standard with an increase in Δρ/ρ in fields higher 0.8 T (Fig. 3a). At temperatures from 40 K to 100 K, such a segment disappears and the Δρ/ρ(B) dependence becomes close to linear dependence on magnetic field, which is not characteristic for semiconductors with a quadratic dispersion of the energy bands [13]. As the sample temperature increases from 150 K and higher, dependences Δρ/ρ(B) approach parabolic ($\Delta\rho/\rho \sim B^2$) dependences, which is confirmed by the appearance of a linear segment on the dependence of Δρ/ρ on the magnetic induction square for both samples at these temperatures (it is not shown). It is interesting that the values of Δρ/ρ at 50 K are higher than they at 300 K by a factor of 25. This fact corresponds to the change in the relative magnetoresistance by 511% for sample **B** at magnetic induction 4 T and temperature 50 K (Fig. 3a). Such a significant increase in the magnetoresistance with a decrease in temperature to 50 K was proved by the temperature–field dependences of the relative magnetoresistance (Fig. 3b).

As temperature decreases to 30 K, an increase in the relative magnetoresistanc significantly decreases, which is due to an increase in the total resistivity of the film and a decrease in the contribution of the hole current of the opposite direction. The CaSi film in sample **E** also demonstrates linear segments of the dependence of Δρ/ρ on the magnetic induction (Fig. 3c) with maximum Δρ/ρ = 180%. At lower temperatures, such a dependence is not observed, and the transition to a parabolic dependence $\Delta\rho/\rho \sim B^2$ takes place at $T = 200$–300 K. The dependence of the resistivity on the magnetic induction is confirmed by its change with magnetic field during cooling the sample (Fig. 3d).

Another character of changing Δρ/ρ with magnetic field is observed for the $CaSi_2$ films in samples **C** and **I** (Fig. 4). In sample **C**, we observe the transition from a zero relative magnetoresistance at $T = 1.4$ K to a positive that with a complex magnetic-field dependence

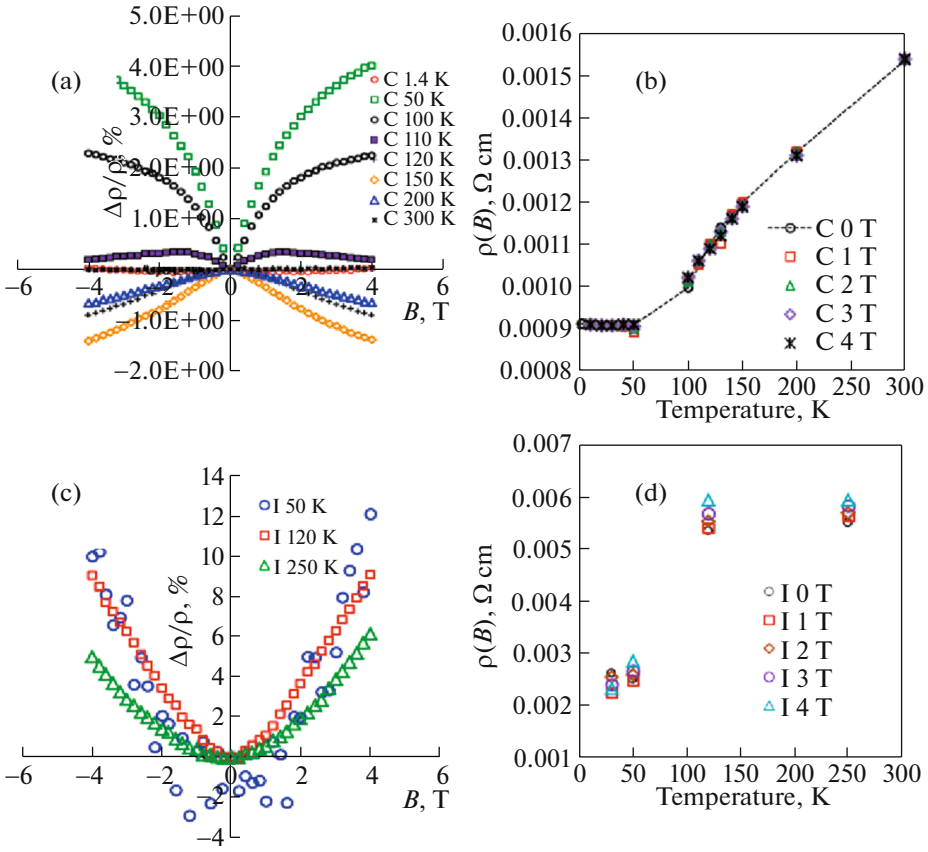

Fig. 4. (a, c) Dependences of the relative change in the magnetoresistance (Δρ/ρ)of the films on the magnitude of the magnetic induction at two directions of the magnetic field and (b, d) the change in the resistivity of the films in zero and nonzero magnetic fields on the temperature in samples **C** and **I** with $CaSi_2$ films.

and saturation at $T = 50–110$ K (Fig. 4a). As temperature increase from 120 K to 200 K, the transition to negative magnetoresistances is observed. The increase in the temperature to 300 K leads once again to a zero value of Δρ/ρ. In the maximum field, the Δρ/ρ values are changed from −1.4% to +4.2% at $B = 4.0$ T, which is susbstantially less than for the CaSi films (Figs. 3a, 3c). The transition to the region of negative magnetoresistance occurs at temperatures 120–150 K as there are bends in the ρ(T) (Fig. 2a) and ρ(B) (Fig. 4b) curves. This result correlates also with the bend in the temperature dependence of the Hall coefficient (Fig. 2a).

Therefore, the specific features of the transport and magnetoresistive properties at low temperatures are related to the realization of phase transitions in nanocrystals of the $CaSi_2$ and CaSi films, since the **C** sample film contains these two phases, according to the XRD data (Table 1). In addition, the peculiarities of three-particle processes (electrons, holes, phonons and their quasiparticles) in the two types of semimetal nanocrystals lead to an increase in the electrical conductivity in magnetic field and the realization of the negative magnetoresistive effect. The latter effect is observed at quite high temperatures, in weak and moderate magnetic fields, thus, it is not related to quantum processes [14].

In the case as the film consists only of $CaSi_2$ nanocrystals with two types of packing calcium and silicon layers (Table 1), as is the case in sample **I** (Fig. 4b), the dependence of the MRE signal are parabolic from 120 K to $T = 300$ K. The decrease in temperature to 50 K leads to an increase in the spread in the values of Δρ/ρ, but the shape remains to be close to parabolic. In this case, the sample resistivity is only slightly dependent on magnetic field to $B = 4$ T (Fig. 4d), and its value sharply decreases at $T = 50$ K.

Thermoelectric Properties of CaSi and $CaSi_2$ Films on Silicon

Consider the data of thermoelectric measurements for the polycrystalline and nanocrystalline CaSi films in samples **A**, **B**, **E**, and **H** and $CaSi_2$ films in samples **C**, **D**, **G**, and **I** (Table 1). Since the films were grown on silicon substrates of two types, the comparison of the data for the films will be performed for each of the substrate types. Figures 5a, 5b show the temperature

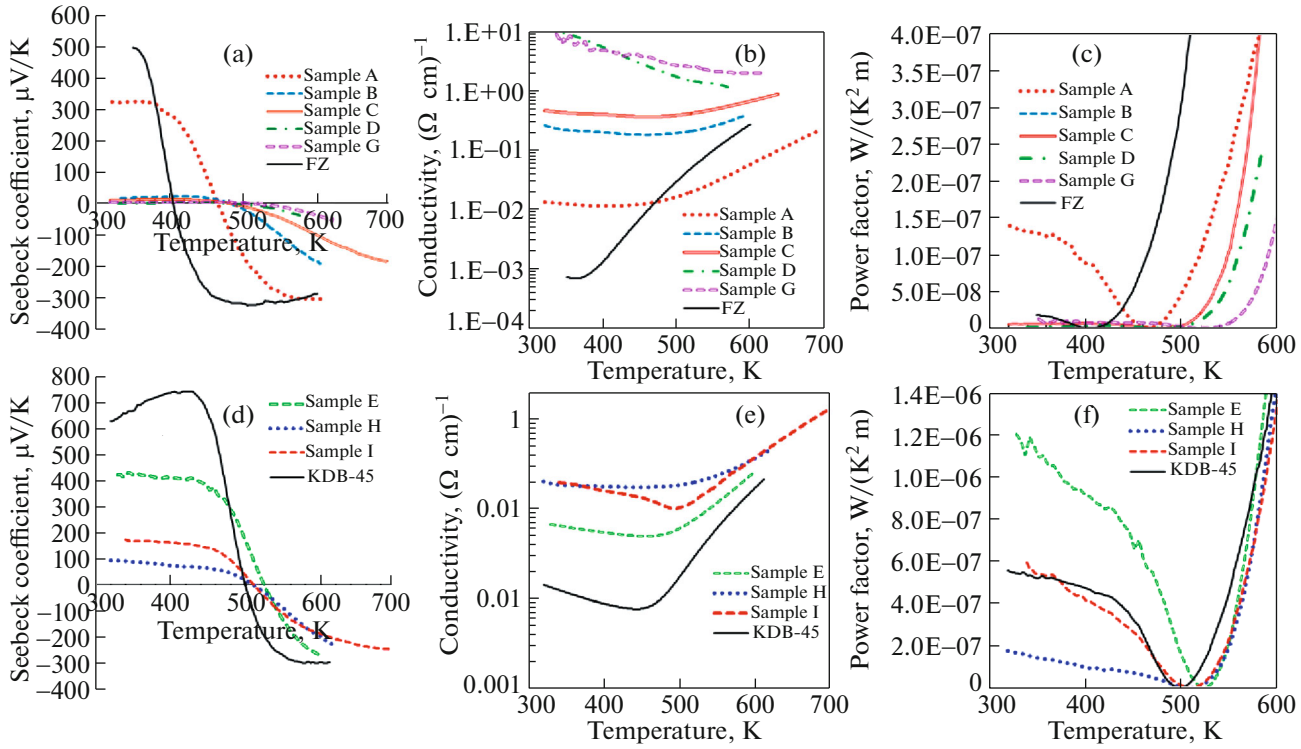

Fig. 5. Temperature dependences of (a, d) the Seebeck coefficient, (b, e) conductivity, and (c, f) power factor for samples **A**, **B**, **C**, **D**, and **G** on an FZ substrate and samples **E**, **H**, and **I** on a KDB-45 substrate.

dependences of the Seebeck coefficient for CaSi films in samples **A**, **B**, and **F** and $CaSi_2$ films in samples **C**, **D**, **G**, and in the FZ-2000 substrate. It is seen that the CaSi and $CaSi_2$ films on the substrate conserve the positive sign of the Seebeck coefficient to temperature no lower than 460 K. In this case, the sign change of the Seebeck coefficient in the FZ substrate is observed at 410 K, which is related to its transition to the region of the intrinsic conductivity and the generation of high density of electrons and holes. The maximum Seebeck coefficient (α = 320 μV/K at T = 335–370 K) is observed for sample **A** with the polycrystalline CaSi film and a small fraction of the amorphous phase of semiconducting Ca_2Si (Table 1), the contribution of which was also identified by the data of the Raman spectroscopy (RS) [9]. The film demonstrates non-silicon character of the temperature dependence of the electrical conductivity (Fig. 5b) and the maximum power factor as compared to silicon at temperatures to 400 K (Fig. 5c).

On the other hand, in the two-phase CaSi film with additional $CaSi_2$ NC crystals (sample **B**), the Seebeck coefficient decreases noticeably (α = 10–15 μV/K at T = 335–460 K). This fact is confirmed by the minimal Seebeck coefficient (Fig. 5a) for the $CaSi_2$ films with additional CaSi phase in samples **C**, **D**, and **G** (Table 1). The existence of the main and additional $CaSi_2$ phase leads to an increase in the electrical conductivity (Fig. 5b) and a sharp decrease in the power factor, which can be related with a competition of two types of carriers as in the $CaSi_2$ phase, so in the CaSi phase. The single-phase amorphous CaSi film with inclusions of CaSi nanocrystals in samples **E** (Table 1) on the KDB-45 substrate shows a marked increase in the Seebeck coefficient to 420 μV/K (Fig. 5d), the increase in the electrical conductivity as compared to that of the substrate (Fig. 5e), and a marked increase in the power factor at temperatures to 500 K (Fig. 5f) even as compared to sample **A** (Fig. 5c).

In the polycrystalline CaSi film with two types of the crystal orientations in sample **H** (Table 1), the Seebeck coefficient decreases to 100 μV/K (Fig. 5d), the electrical conductivity increases markedly (Fig. 5e), and the power factor decreases by a factor of six (Fig. 5f) as compared to sample **E**. In the $CaSi_2$ film consisting of two polytypes of $CaSi_2$ crystals (hR3 and hR6, Table 1), the Seebeck coefficient increases to 170 μV/K (Fig. 5d), the conductivity increases as compared to that of silicon (Fig. 5e), and the power factors are close to that of silicon in the range from 430 to 500 K (Fig. 5f).

CONCLUSIONS

The correlation of the grain morphology, low-temperature, Hall and magnetoresistive effects, and also-

high-temperature thermoelectric carrier generation has been studied in calcium silicide films grown on high-resistance silicon substrates with orientations (111) and (100) using to low-temperature methods (190–330°C): molecular beam and solid-phase epitaxies. The low-temperature Hall measurements of polycrystalline, nanocrystalline (NC), and amorphous CaSi and $CaSi_2$ films on Si(100) and Si(111) substrates showed that all the systems under study are characterized by a preferential contribution of holes in the range 1.4–300 K. For the CaSi films with additional $CaSi_2$ phase, the giant linear magnetoresistive effect (MRE, 200–500%) in magnetic fields 1–4 T at $T = 40$–100 K was observed for the first time. In the $CaSi_2$ films with additions NC CaSi, we detected the effect of the formation of peaks on the temperature dependences of the resistivity and the Hall coefficient that can be determined by the formation of phase transitions. The existence of CaSi nanocrystals in the $CaSi_2$ film also causes the transition from the positive MRE to negative MRE at $T = 120$–200 K that correlates with the resistivity maximum and the features in the Hall coefficient function. This effect was mot observed in the single-phase $CaSi_2$ film at temperatures from 50 K to 250 K, which allows us to conclude that, in the two-phase system, a certain reconstruction of carrier flows in magnetic field takes place. The semimetallic conduction type in the CaSi and $CaSi_2$ films is shown to lead to the independence of the positive Seebeck coefficient at $T = 330$–450 K. The maximum Seebeck coefficient and power factor are observed in the case of the single-phase CaSi amorphous film with some fraction of Ca_2Si NC phase. In the case of the single-phase polycrystalline $CaSi_2$ film with two polytypes of the same orientation hR3-$CaSi_2$(001) and hR6-$CaSi_2$(001), the Seebeck coefficient and the power factor are halved.

ACKNOWLEDGMENTS

The authors are grateful to the Chair of functional nanosystems and high-temperature materials of National Research and Technology University MISiS for the chance to perform the thermoelectric measurements on their experimental equipment.

FUNDING

This work was supported by the Russian Foundation for Basic Research, project no. 19-02-00123_a.

REFERENCES

1. P. Manfrietti, M. L. Fornasini, and A. Palenzona, Intermetallics **8**, 223 (2000). https://doi.org/10.1016/S0966-9795(99)00112-0
2. S. Lebegue, Phys. Rev. B **72**, 085103 (2005).
3. O. Bisi, L. Braikovich, C. Carbone, I. Lindau, A. Iandelli, G. L. Olcese, and A. Palenzona, Phys. Rev. B **40**, 10194 (1989).
4. S. Fahy and D. R. Hamann, Phys. Rev. B **41**, 7587 (1990).
5. M. Affronte, O. Laborde, G. L. Olsece, and A. Palenzona, J. Alloys Compd. **274**, 68 (1998).
6. J. Tani and H. Kido, Comput. Mater. Sci. **97**, 36 (2015).
7. N. G. Galkin, K. N. Galkin, A. V. Tupkalo, D. L. Goroshko, E. A. Chusovitin, Z. Fogarassy, and B. Pécz, Jpn. J. Appl. Phys. **59**, SFFA12 (2020).
8. N. G. Galkin, K. N. Galkin, A. V. Tupkalo, S. A. Dotsenko, Z. Fogarassy, and B. Pécz, Int. J. Nanosci. **18**, 1940014 (2019).
9. N. G. Galkin, K. N. Galkin, I. M. Chernev, D. L. Goroshko, E. A. Chusovitin, A. V. Shevlyagin, A. A. Usenko, and V. V. Khovailo, Dif. Def. Forum **386**, 3 (2018).
10. N. G. Galkin, S. A. Dotsenko, K. N. Galkin, D. B. Migas, V. O. Bogorodz, A. B. Filonov, V. E. Borisenko, I. Cora, B. Pécz, D. L. Goroshko, A. V. Tupkalo, E. A. Chusovitin, and E. Y. Subbotin, J. Alloys Compd. **770**, 710 (2019).
11. E. C. Reyes and R. Nesper, J. Phys. Chem. C **116**, 2536 (2012).
12. L. Schnatmann, K. Geishendorf, M. Lammel, C. Damm, S. Novikov, A. Thomas, A. Burkov, H. Reith, K. Nielsch, and G. Schierning, Adv. Electron. Mater. **6**, 1900857 (2020). https://doi.org/10.1021/jp205825d
13. Y. P. Yu and M. Cardona, *Fundamental of Semiconductors: Physics and Materials Properties,* 4th ed. (Springer, Heidelberg, 2010). https://doi.org/10.1002/aelm.2019008
14. A. A. Abrikosov, Europhys. Lett. **49**, 789 (2000).

Translated by Yu. Ryzhkov